J Nanostruct 16(2): 1686-1696, Spring 2026

RESEARCH PAPER

Preparation and Characterization of Chromium Oxide Nanoparticle for Environmental Applications

*Hiba R. Kazem [1], Hadeer Mohammed Subhi [2], Hazim Y. Al-gubury [2] *, Karam Khadhim [2], Fatam Abdullah Omran [3]*

[1] *Department of Chemistry, College of Science, University of Babylon, Hilla, Iraq*

[2] *Department of Chemistry, College of Science for Women, University of Babylon, Hilla, Iraq*

[3] *Medical Laboratory Techniques Department, College of Health and Medical Techniques, Al-Mustaqbal University, Babylon, Iraq*

ARTICLE INFO

Article History:
Received 02 December 2025
Accepted 28 February 2026
Published 01 April 2026

Keywords:
Chromium oxide NP
Cracking
Malachite green dye
Nanoparticles
Photo degradation

ABSTRACT

This article uses produced nanoparticles and a UV lamp to study the photocatalytic degradation process of the malachite green dye... sol-gel precipitation route was used to create the chromium oxide nanoparticles. The first part includes the preparation of chromium oxide nanoparticles using the sol-gel precipitation route. X-ray diffraction (XRD) was used to investigate the properties of nanocomposite materials. The particle size of synthesized chromium oxide nanoparticles was determined using the Scherer equation. Dye degradation was conducted in irradiated aqueous suspension solutions, utilizing 0.17 g/100 ml of nanocomposite, with varying dye concentrations. The impact of nanocomposite mass, Malachite-green-dye concentration and temperature on the photocatalytic degradation of Malachite-green dye was investigated. The calculated activation energy is 38.61 kJ.mol-1. The irradiation solutions were examined using a UV-Vis spectrophotometer.

How to cite this article
Kazem H., Subhi H., Al-gubury H., Khadhim K., Omran F. Preparation and Characterization of Chromium Oxide Nanoparticle for Environmental Applications. J Nanostruct, 2026; 16(2):1686-1696. DOI: 10.22052/JNS.2026.02.021

INTRODUCTION

Water Contamination refers to the deterioration of water quality caused by harmful substances making it unsafe for consumption, agriculture, hygiene, and ecosystem health. According to the World Health Organization, contaminated water is that which has been altered to such an extent that it becomes unusable, often causing severe illnesses like cholera, dysentery, typhoid, and hepatitis, which claim hundreds of thousands of lives annually, Causes of water contamination stem from both human activity and natural processes[1- 3].Agricultural runoff: includes fertilizers, pesticides, and animal waste that enter rivers and groundwater, causing nutrient pollution and algal blooms. Industrial discharge: chemicals and heavy metals improperly released into water bodies contaminate them with toxic substances Sewage and wastewater: untreated or poorly treated sewage introduces pathogens and pollutants into freshwater systems. Urbanization and poor waste management: plastics, leachate, and household trash penetrate water supplies in rapidly growing cities. Natural events: storms,

* *Corresponding Author Email: h.yahya40@yahoo.com*

flooding, or mineral leaching can mobilize sediments and raw pollutants into water sources.

Advanced Oxidation Processes (AOPs) denote a collection of chemical treatment methods aimed at eliminating organic and inorganic contaminants from water and air. These processes utilize highly reactive species, mainly hydroxyl radicals (•OH), to break down contaminants into harmless end products such as water and carbon dioxide. Various methods are employed for wastewater treatment, typically categorized into physical, chemical and biological techniques [4]. Regrettably, numerous procedures are expensive, produce environmentally detrimental by-products, and exhibit complexity. Because of their effectiveness, characteristics, and advantages, advanced oxidation processes (AOPs), especially photo catalysis, are among the most widely used technologies for treating these effluents [5]. Photo catalysis has proven to be incredibly simple, economical, and efficient. Because of its effectiveness in breaking down organic contaminants like industrial colors, it has attracted a lot of research interest [6,7]. The approach is advantageous and secure, as it effectively purifies water containing certain color pollutants without producing harmful intermediate products in the majority of instances [8]. These semiconductor nanoparticles can produce electron-hole pairs [9] when exposed to light at a particular wavelength. These pairs then take part in a sequence of oxidation and reduction reactions, producing hydroxyl groups as the main oxidizing agent and aiding in the breakdown of the dye's organic components into products that are safe for the environment [10].

An organic substance called malachite green is employed in aquaculture as a color and, more controversially, as an antibacterial agent. Malachite is commonly used as a dye for materials such as silk, leather, and paper; however, despite its name, the dye is not derived from the mineral malachite; the name simply refers to the color similarity. In the dye industry, malachite green is categorized as a triarylmethane dye; it is also utilized in the pigment industry [11]. Although the name is commonly used more broadly to refer only to the colored cation, malachite green technically refers to the chloride salt $[C_6H_5C(C_6H_4N(CH_3)_2)_2]$ Cl. Cotton, silk, wool, leather, and paper are all colored with a synthetic dye called malachite green (di[4-dimethylamino-phenyl] phenyl cation). In the aquaculture industry, malachite green is a topical fungicide that works well. Malachite green (MG) is a green, metal-based triphenylmethane fertilizer that poses a serious risk to water quality [12]. The molecule is significantly more reactive when the benzene ring is present. It poses a serious risk to human life and health and can result in cancer and cell apoptosis [13].

MATERIALS AND METHODS

Chromium chloride hex hydrate salt ($CrCl_3•6H_2O$) supplied by Fluke, Ethanol (EtOH) supplied by Fluke, Ammonium hydroxide (NH4OH) supplied by Fluke, Every chemical was used

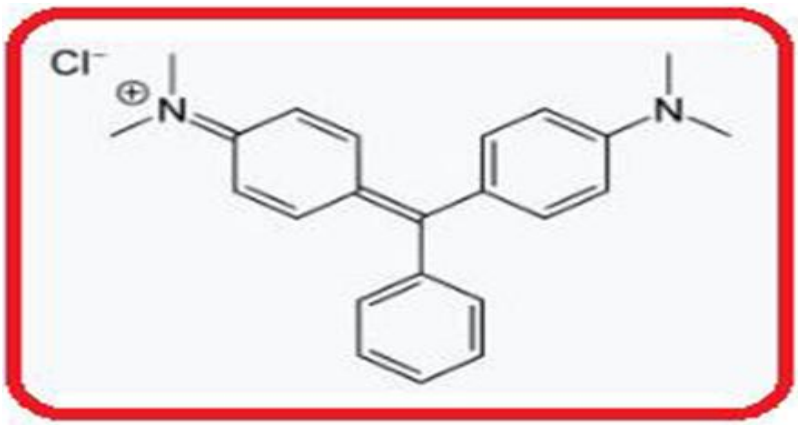

Fig. 1. The chemical structure of the malachite green dye.

without any additional purification.

Synthesis of Chromium oxide (Cr_2O_3) nanoparticles

Chromium oxide (Cr_2O_3) nanoparticles have been synthesized via the technique of sol-gel method. In 50 milliliters of ethanol (EtOH), around 2 grams (7,5 mmol) of chromium chloridhexahydrate ($CrCl_3.6H_2O$) was dissolved. After being shaken in a container on a magnetic stirrer for about half an hour, the resultant solution became green.

The resulting solution was then gradually supplemented with ammonium hydroxide solution (NH_4OH) using a burette at a rate of around two drops per minute until the pH reached about 8. Ten minutes later, the solution was filtered through a centrifuge, the over stands were taken off, and the solution was washed twice with a little amount of distilled water. The precipitate was then dried for two hours at 90 °C. The chromium oxide precipitate powder, which was dark green, was obtained.

Malachite green dye is broken down by photo catalysis using chromium oxide nanoparticles

In degradation studies, chromium oxide (Cr_2O_3) nanoparticles were used as a photo catalyst to break down malachite green dye in aqueous solution when exposed to UV light as shown in Fig. 2. The suspension solution was chilled by circulating cooling water through the first apparatus. A 100 mL dye degradation suspension solution makes up the second component. Malachite green dye was prepared as a 100 ppm stock solution using distilled water. For every

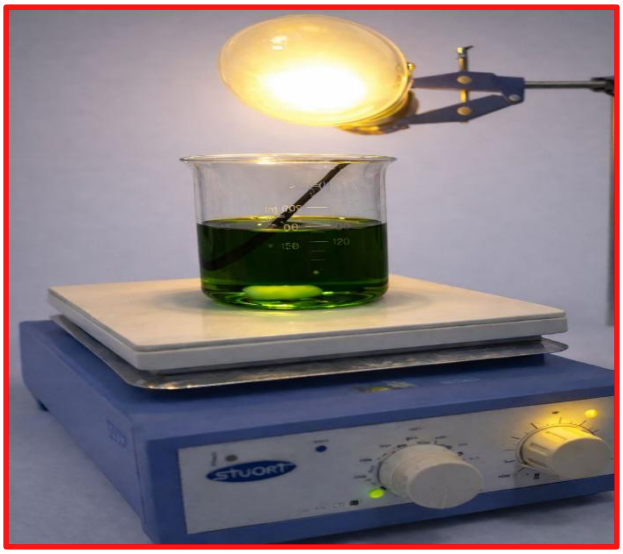

Fig. 2. Malachite green dye degradation by photo catalysis using the system of the photocatalytic cell.

Table 1. Crystalline size and lattice parameter of the prepared chromium oxide nanoparticles

2θ	Miller indices	Crystalline size
26.0844°	012	29.91992
31.2530°	104	34.74132
37.6206°	006	30.60786
40.0649°	113	31.18837
46.2634°	202	29.60308
54.2889°	116	27.95518
64.9477°	122	33.54621
66.5431°	214	24.54362

color concentration, a suspension solution was created by stirring. One hundred milliliters of each 0.17 g of chromium oxide nanoparticles were added to the liquid to amalgamate the hue, and it was then shaken. The matching suspension solution combination has been irradiated using an ultraviolet light source. A syringe was used to extract 2-3 mL of each sample every 10 minutes. After centrifuging the samples for ten minutes at 3000 rpm, a UV-Vis spectrophotometer was used to test each sample's absorbance.

RESULTS AND DISCUSSION

X-ray diffraction of synthesized chromium oxide:

Fig. 3. shows the XRD pattern of synthesized chromium oxide nanoparticle, and explain the main bands which parallel to chromium oxide were observed having 2θ values of 21.3826°, 26.0844°, 31.2530°, 37.6206°, 40.0649°, 46.2634°, 52.4677°, 54.2889°, 64.9477°, 66.5431°, and 69.3505°, corresponds to the (012), (104), (110), (006), (113), (202), (024), (116), (122), (214), (300) and (101) planes of Cr_2O_3 (JCPDS Card No. 72-3533) respectively [14,15].

X-ray diffraction reveals that the produced Nano metal oxide is 100% Cr2O3 and has a hexagonal form. The oxide nanoparticles' good crystal formation is indicated by the peaks' sharpness. The average particle size (D) of the particles was calculated from the high intensity peak using the Debye-Scherer equation [16]:

$$D = K\lambda / (\beta cos\theta)$$

where D is the crystalline size of the Nano powders of chromium oxide.

K is equal to 0.89, β is the line width at half-maximum height (FWHM), θ is the Bragg's angle, and λ mean is the wavelength of the X-ray radiation, which is equal to (λ=0.15406 nm) for CuKα. Table 1 shows the crystalline size of chromium oxide.

Scanning Electron Microscopy (SEM) for synthesized Cr_2O_3 nanoparticle

The morphology of the created Cr_2O_3 nanoparticle was analyzed using scanning electron microscopy techniques (SEM, Zeiss, Germany) in order to obtain crucial information about its structure. SEM images. As illustrated in Fig. 4. The SEM micrograph shows a highly agglomerated morphology composed of numerous fine nanoparticles distributed densely across the surface [17]. The particles exhibit predominantly spherical to nearly spherical shapes, forming

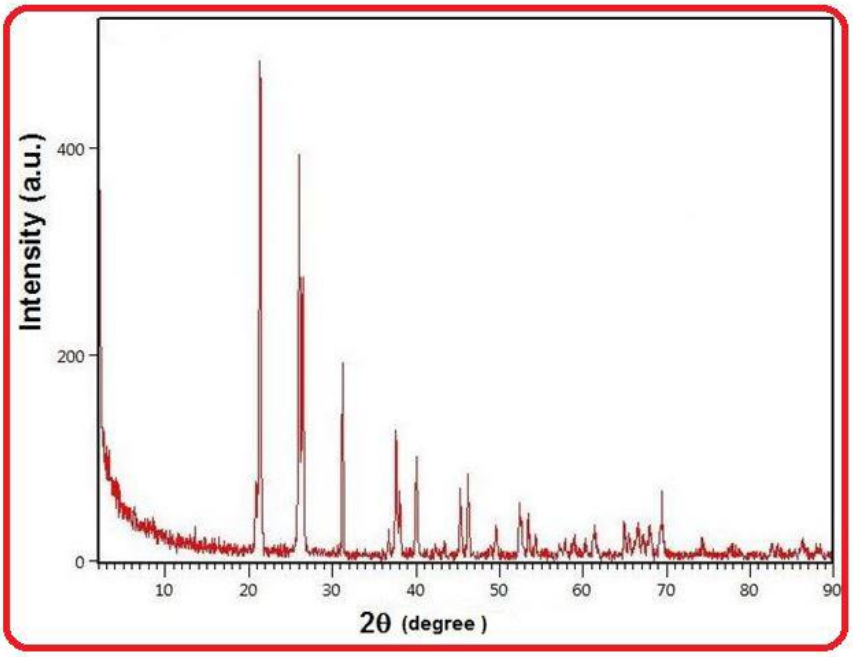

Fig. 3. shows the XRD pattern of the produced Cr_2O_3 powder.

irregular clusters due to aggregation, which is common in nanoscale metal oxides because of their high surface energy. The image, taken at a magnification of 2500×, reveals that the material has a rough and porous surface texture, indicating a large surface area. This type of morphology is beneficial for applications such as photo catalysis, adsorption, and sensing, as the high surface area enhances active site availability. The uniform distribution of the nanoparticles also suggests that the synthesis method produced a relatively consistent particle formation without large micro-

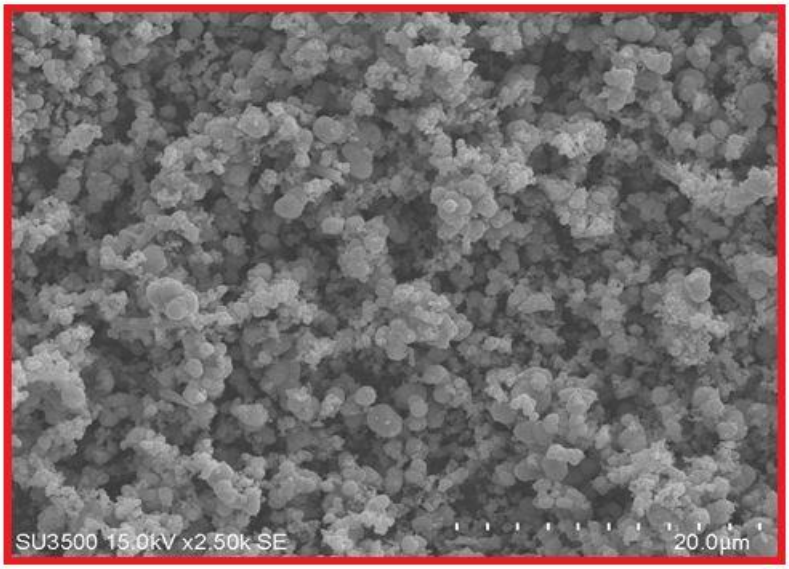

Fig. 4. SEM pattern of Cr_2O_3 nanoparticle.

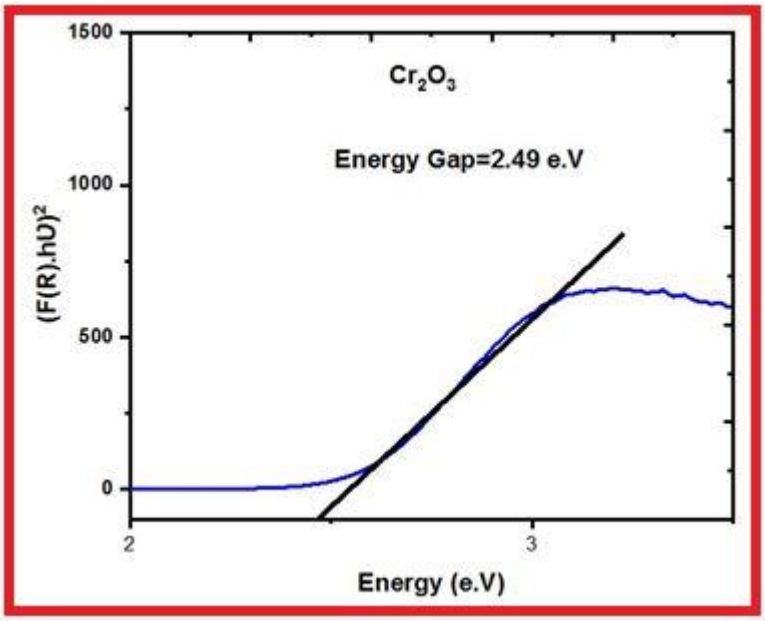

Fig. 5. The band gap from Cr_2O_3 nanoparticle.

sized impurities [18,19].

Band Gap Energy of Cr_2O_3 nanoparticle

The plot shows the relationship between ((F(R). hν)²) and the photon energy (hν) Fig. 5, where (F(R)) is the Kubelka–Munk function derived from the UV–Vis diffuse reflectance data. In this analysis, the exponent n = 2 is used, indicating that Cr_2O_3 is treated as a material with a direct allowed electronic transition[20].The linear portion of the curve in the higher-energy region is extrapolated toward the energy axis (x-axis). The point where

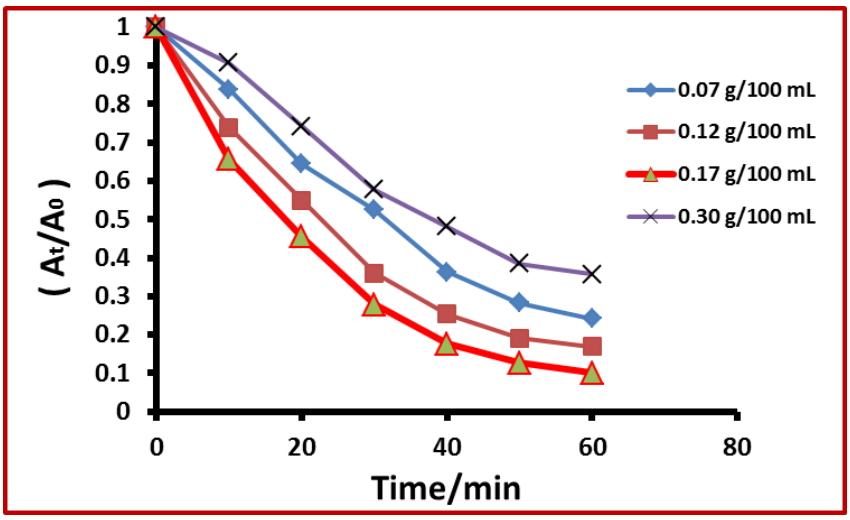

Fig. 6. Change in (At/A0) with the irradiation period of the generated dye at 40 mg/L.

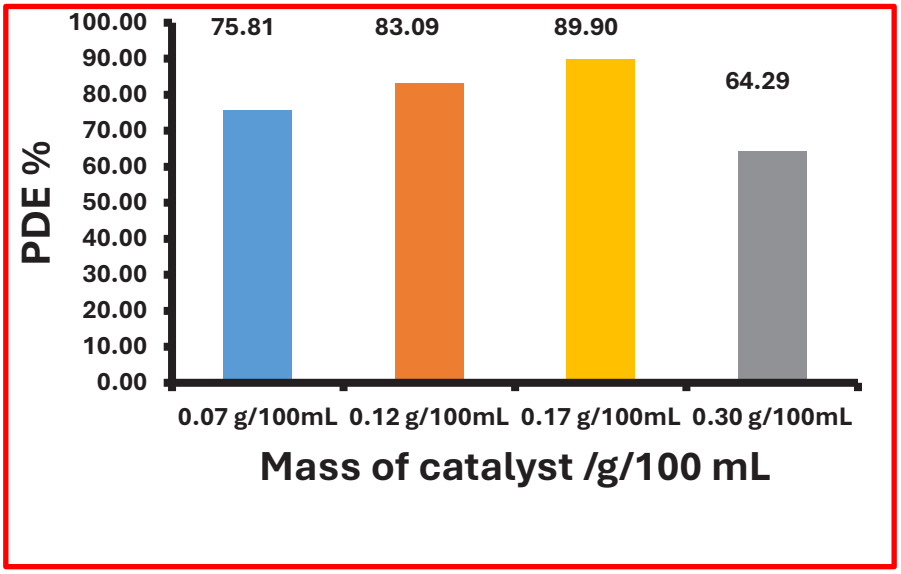

Fig. 7. Photocatalytic degradation efficiency using 0.17g/100 mL of chromium oxide nanoparticles and 40 ppm of malachite green dye.

the extrapolated straight line intersects the x-axis corresponds to the optical band gap energy (E_9). From the extrapolation shown in the figure, the estimated band gap of Cr_2O_3 is: Eg = 2.49 Ev.

The energy needed for electrons to move from the valence band to the conduction band is represented by this value. A band gap of approximately 2.49 eV indicates that Cr_2O_3 can absorb visible light and is suitable for applications such as photocatalysis, sensors, pigments, and

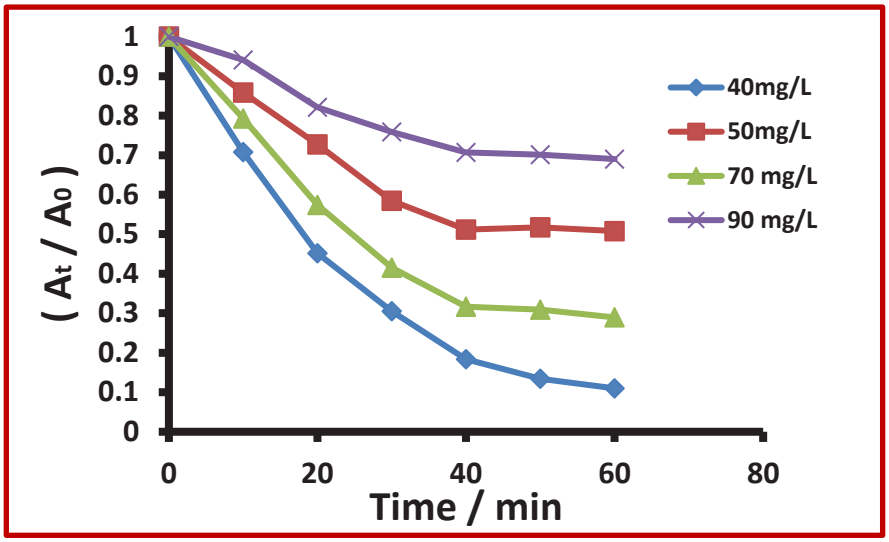

Fig. 8. Variations in (At/A0) at different dye concentrations with time and irradiation:

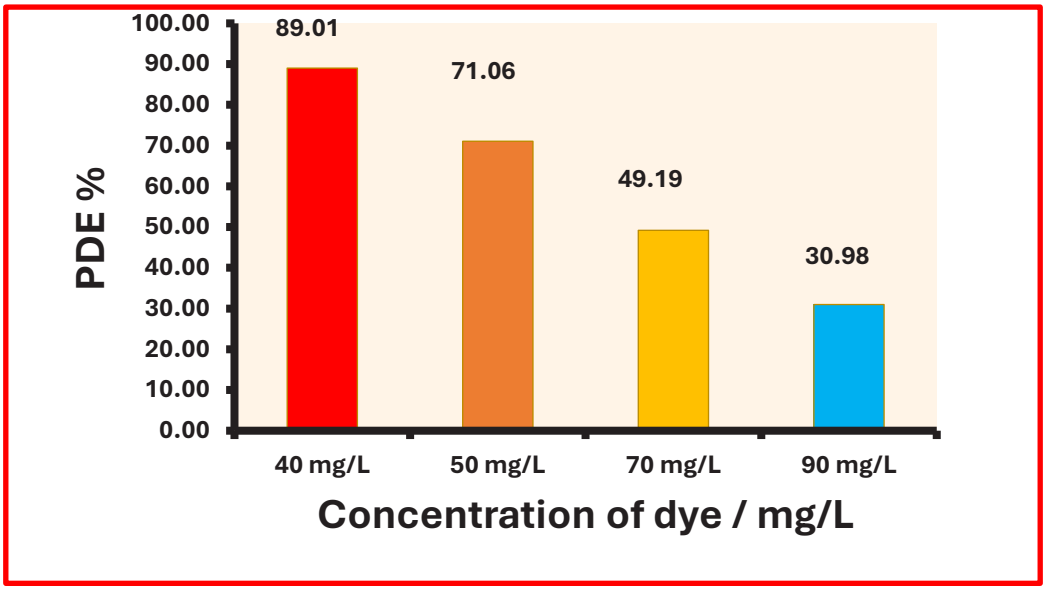

Fig. 9. The effectiveness of photocatalytic degradation using 0.17g/100 mL of chromium oxide nanoparticles and 40 ppm of malachite green dye.

optoelectronic devices[21,22].

Effect of loaded mass of Chromium oxide nanoparticles on the Malachite green dye's photocatalytic degradation

Using a dye concentration of 40 mg/L, an air flow rate of 10 mL/min, and at room temperature, the effect of chromium oxide nanoparticle mass on the photocatalytic degradation of malachite green dye was investigated. As the mass of chromium oxide nanoparticles increases to as seen in Figs. 6 and 7, the photocatalytic degradation of Malachite Green dye starts at 0.17 g/100 ml, climbs steadily, and then progressively diminishes. with a mass of 0.17 g/100 ml of chromium oxide nanoparticles. The semiconductor has the capacity to absorb the lightest possible. Only at concentrations of chromium oxide nanoparticles more than 0.17 g/100 ml will the primary layers of malachite green dye experience a reduction in photo degradation efficiency as a result of light absorption; the solution's subsequent phases are not exposed to light photons. This effect was studied by several researchers 23]. The rate of photo degradation of malachite green dye also decreases when the loading mass of chromium oxide nanoparticles is below the optimal value of 0.17 g/100 ml. This is because the mass of the nanoparticles' surface area decreases, which lowers the amount of light that the nanoparticles can absorb [24].

Impact of starting concentration of malachite green dye on photocatalytic degradation

The effects of the concentration solution of malachite green dye by maintaining constant conditions throughout, the experiment investigated the spectrum of photocatalytic degradation processes (40-90 mg/L). Fig. 8 presents a graphical representation of the findings. Our findings showed that when the initial dye concentration rose, the rate of photocatalytic degradation reduced. The number of photons that come into touch with the catalyst surface increases as the concentration of Malachite green dye drops because the photon's journey lengthens as it enters the solution. This speeds up the production of superoxide ions and hydroxyl radicals, which in turn speeds up the rate at which materials degrade [25,26].

The high photo degradation efficiency (89.01%) was 40 mg/L when the quantity of malachite green dye was enough. The photocatalytic degradation efficiency (P.D.E.) at different concentrations of malachite green dye is shown in Fig. 9.

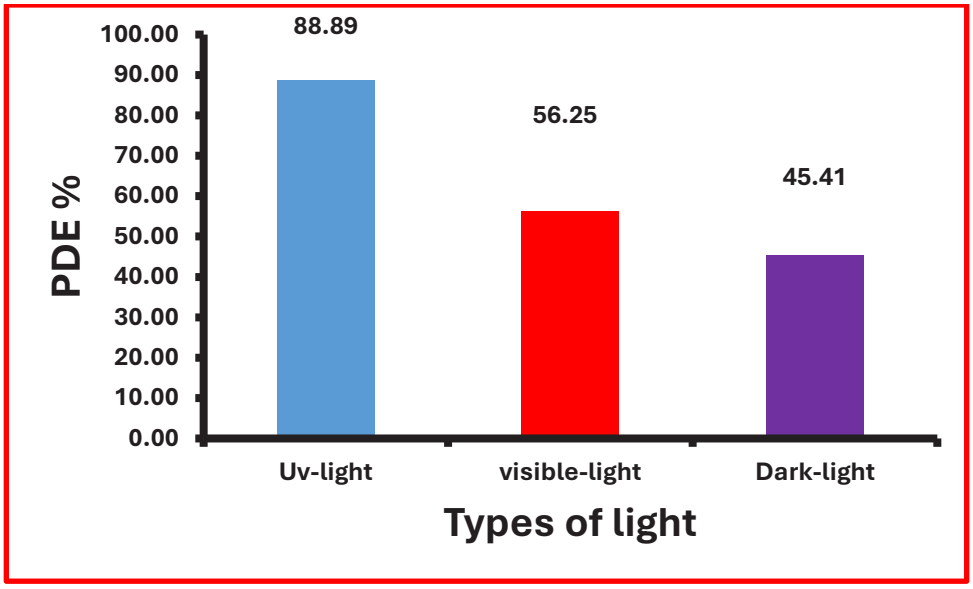

Fig. 10. The effectiveness of photocatalytic degradation employing 0.17g/100 mL of chromium oxide nanoparticles and 40 ppm of malachite green dye under various light conditions.

The Impact of Light Irradiation Type:

Fig. 10 illustrates how different forms of light irradiation affect the breakdown of malachite green dye. 88.89% of the dye destroyed under UV light in 60 minutes, whereas 56.25% and 45.41 percent of the dye decomposed under visible light in 60 minutes, respectively. This finding indicates that the degradation of malachite green dye was not significantly impacted by either visible or dark light. The experiment also examined the weak

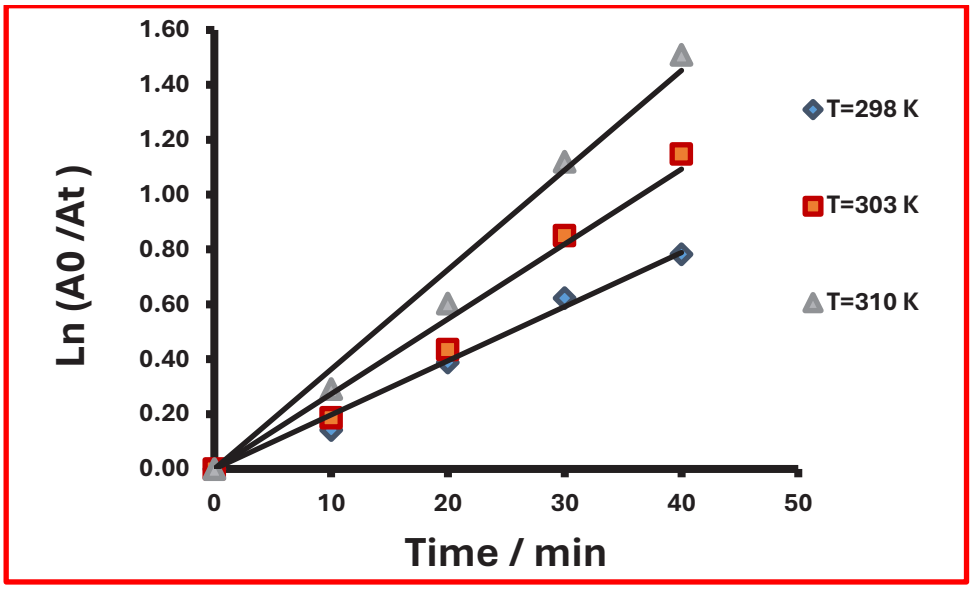

Fig. 11. The change in ln (At/A0) with temperature and UV radiation exposure duration. The starting concentrations of Malachite green dye were 40 mg/L, and the levels of photo catalyst were 0.17 g/100 mL.

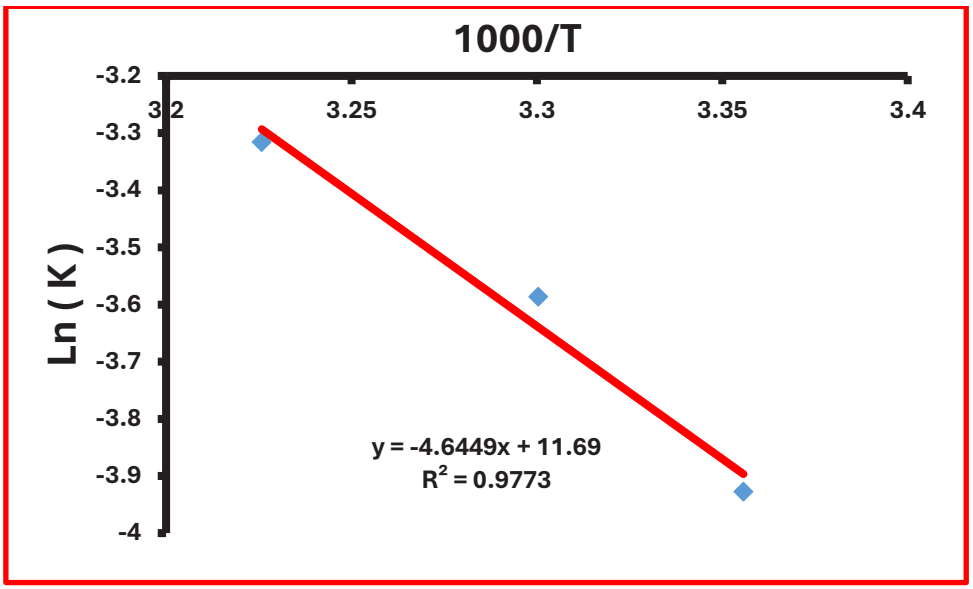

Fig. 12. Malachite green dye Arrhenius plot.

adsorption mechanism between chromium oxide nanoparticles and malachite green dye in a dark environment [27].

The effect of temperature on the photocatalytic degradation of malachite green dye

The effects of temperature on the photocatalytic degradation of malachite green dye were examined using a range of tests from 298 to 310 K. With all testing settings held constant, the created amount of chromium oxide nanoparticle catalyst was 0.17 g per 100 mL, whereas the initial concentration of malachite green dye was 40 ppm.

The results in Fig. 11 demonstrate that the dye's degradation accelerated with temperature. The existence of more reactive hydroxyl radicals might be the cause of this [28-32]. Plotting Fig. 12 illustrates The Arrhenius equation was used to calculate the activation energy related to dye photo degradation in k versus 1/T, and the result was 38.61kJ.mol^{-1}.

CONCLUSION

Hexagonally structured chromium oxide nanoparticles have been synthesized utilizing the sol-gel method. The prepared sample was analyzed via the X-ray diffraction method. This article employed a co-precipitation approach to synthesize chromium oxide nanoparticles. The optimal concentration of chromium oxide nanoparticles was found to be 0.17 g per 100 mL. The catalyst dosage dictated the photocatalytic degradation of malachite green dye. The effects of malachite green dye on dye concentration have been studied at the ideal dosage of 40 mg/L. Because there is less OH^- adsorption on the catalyst surface, the rate of photocatalytic degradation decreases as the amount of Malachite green dye increases. The efficiency of the photocatalytic degradation of malachite green -farbstoff is 89.01 percent. The activation energy, according to calculations, is 38,61 kJ•mol^{-1}.

ACKNOWLEDGMENTS

We would like to thank the University of Babylon and the Chemistry Department of the Faculty of Science for Women and College of science for their help in making this project successful.

CONFLICT OF INTEREST

The authors declare that there is no conflict of interests regarding the publication of this manuscript.

REFERENCES

1. Neethu N, Choudhury T. Treatment of Methylene Blue and Methyl Orange Dyes in Wastewater by Grafted Titania Pillared Clay Membranes. Recent Patents on Nanotechnology. 2018;12(3):200-207.
2. Safavi-Mirmahalleh S-A, Salami-Kalajahi M, Roghani-Mamaqani H. Adsorption kinetics of methyl orange from water by pH-sensitive poly(2-(dimethylamino) ethyl methacrylate)/nanocrystalline cellulose hydrogels. Environmental Science and Pollution Research. 2020;27(22):28091-28103.
3. Subhi HM, Bader AT, Al-Gubury HY. Synthesis and Characterization of ZnO Nanoparticles via Thermal Decomposition for Zn(II) Schiff Base Complex. Indonesian Journal of Chemistry. 2022;22(5):1396.
4. Peerakiatkhajohn P, Yun J-H, Butburee T, Lyu M, Takoon C, Thaweesak S. Dual functional WO_3/$BiVO_4$ heterostructures for efficient photoelectrochemical water splitting and glycerol degradation. RSC Advances. 2023;13(27):18974-18982.
5. Abass AK, Raoof SD. Advanced Oxidation Process treatment for azo dyes pollutants using ultra-violet irradiation. Journal of Physics: Conference Series. 2020;1664:012066.
6. Garrido-Cardenas JA, Esteban-García B, Agüera A, Sánchez-Pérez JA, Manzano-Agugliaro F. Wastewater Treatment by Advanced Oxidation Process and Their Worldwide Research Trends. International Journal of Environmental Research and Public Health. 2019;17(1):170.
7. Pandey GP, Singh AK, Deshmukh L, Asthana A, Deo SR. Photocatalytic degradation of an azo dye with ZnO nanoparticles. AIP Conference Proceedings: AIP; 2013.
8. Peerakiatkhajohn P, Butburee T, Sul J-H, Thaweesak S, Yun J-H. Efficient and Rapid Photocatalytic Degradation of Methyl Orange Dye Using Al/ZnO Nanoparticles. Nanomaterials. 2021;11(4):1059.
9. Photocatalytic Degradation of a Textile Dye under UV and Solar Light Irradiation Using TiO_2 and ZnO nanoparticles. International Journal of Advances in Chemical Engineering and Biological Sciences. 2016;3(2).
10. Lim NYY, Chiam SL, Leo CP, Chang CK. Recent modification, mechanisms, and performance of zinc oxide-based photocatalysts for sustainable dye degradation. Hybrid Advances. 2024;7:100318.
11. Xu Z, Zada N, Habib F, Ullah H, Hussain K, Ullah N, et al. Enhanced Photocatalytic Degradation of Malachite Green Dye Using Silver–Manganese Oxide Nanoparticles. Molecules. 2023;28(17):6241.
12. Elkady MF, Hassan HS. Photocatalytic Degradation of Malachite Green Dye from Aqueous Solution Using Environmentally Compatible Ag/ZnO Polymeric Nanofibers. Polymers. 2021;13(13):2033.
13. Amigun AT, Adekola FA, Tijani JO, Mustapha S. Photocatalytic degradation of malachite green dye using nitrogen/sodium/iron-TiO_2 nanocatalysts. Results in Chemistry. 2022;4:100480.
14. Rasheed RT, Easa HA, Jassim LS. Preparation and characterization of Cr_2O_3 nanoparticle prepared by chemical method. AIP Conference Proceedings: AIP Publishing; 2020.
15. Green Synthesis of Silver Nanoparticles by Using Tinospora Cordifolia Stem Powder, Characterization and

Its Antibacterial Activity Against Antibiotics Resistant Bacteria. International Journal of Pharmacy Research and Technology. 2019;3(2).
16. Kothari R, Soni A. Green Synthesis of Chromium Oxide Nanoparticles Using Chromium (Iii) Complex As A Single Route Precursor: Anti-Oxidant Activity. Rasayan Journal of Chemistry. 2022;15(02):1325-1339.
17. Dhami HS, Viswanathan K. Investigating particle morphology, quality, flowability and performance of abrasive-grinding based powders for directed energy deposition. Powder Technol. 2024;437:119533.
18. Malashin I, Martysyuk D. Powder particle classification with scanning electron microscopy images using machine learning techniques. Expert Systems with Applications. 2025;286:128001.
19. Thuan ND, Cuong HM, Nam NH, Lan Huong NT, Hong HS. Morphological analysis of Pd/C nanoparticles using SEM imaging and advanced deep learning. RSC Advances. 2024;14(47):35172-35183.
20. Liu Y, Mo Y. Learning from models: high-dimensional analyses on the performance of machine learning interatomic potentials. npj Computational Materials. 2024;10(1).
21. Sahoo PK, Rajput N, Pal A, Kumar R. Editorial: Wide-bandgap oxide semiconductors: unveiling excitonic potential. Frontiers in Materials. 2025;12.
22. Zhang Z, Song H, Ji Y, Cui Y, Li X, Zhang Z, et al. MELRSNet for accelerating the exploration of novel ultrawide bandgap semiconductors. Microstructures. 2025;5(2).
23. Hade BR, Kazem HR, Al-Mamoori SA, Hussein EK. The Role of Vegetable Oils in Modifying Lipid Profiles in Patients with Non-Alcoholic Fatty Liver Disease. International Journal on Advanced Science, Engineering and Information Technology. 2025;15(5):1569-1574.
24. Kazem HR, Al-Gubury HY. Removal of orange G dye using prepared GO/ZnO nanocomposite as a photocatalyst under solar light irradiation. AIP Conference Proceedings: AIP Publishing; 2023. p. 020006.
25. ANNA. Schweizerische Ärztezeitung. 2014;95(25):ANNA-ANNA.
26. Mathur S, Gautam V, Kumari S, Mishra P. Photocatalytic Degradation of Organic Dye Pollutants Using ZnO Nanoparticles Synthesized from Plumeria alba L. Leaf Extract. SSR Institute of International Journal of Life Sciences. 2024;10(1):3734-3742.
27. Peerakiatkhajohn P, Yun J-H, Butburee T, Chen H, Thaweesak S, Lyu M, et al. Bifunctional photoelectrochemical process for humic acid degradation and hydrogen production using multi-layered p-type Cu2O photoelectrodes with plasmonic Au@TiO_2. J Hazard Mater. 2021;402:123533.
28. Kalaycıoğlu Z, Özuğur Uysal B, Pekcan Ö, Erim FB. Efficient Photocatalytic Degradation of Methylene Blue Dye from Aqueous Solution with Cerium Oxide Nanoparticles and Graphene Oxide-Doped Polyacrylamide. ACS Omega. 2023;8(14):13004-13015.
29. Al-Gubury HY, Alteemi HS, Saad AM, Al-Shamary RR. Removal of Hazardous Brilliant Cresyl Blue Dye Utilizing Aluminum Oxide as Photocatalyst. Indonesian Journal of Chemistry. 2019;19(2):292.
30. Kzar KO, Mohammed ZF, Saeed SI, Ahmed LM, Kareem DI, Hadyi H, et al. Heterogeneous photo-decolourization of cobaltous phthalocyaninate dye (reactive green dye) catalyzed by ZnO. AIP Conference Proceedings: AIP Publishing; 2019. p. 020004.
31. Aa O. Kinetic Study of Decolorization of Methylene Blue with Sodium Sulphite in Aqueous Media: Influence of Transition Metal Ions. Journal of Physical Chemistry and Biophysics. 2014;2(2).
32. Impact on the Photocatalytic Dye Degradation of Morphology and Annealing-Induced Defects in Zinc Oxide Nanostructures. American Chemical Society (ACS).